Herkese Açık

Pamukkale Univ Muh Bilim Derg, XX(X), XX-XX, 20XX

Pamukkale Üniversitesi Mühendislik Bilimleri Dergisi

Pamukkale University Journal of Engineering Sciences

An approach to estimation of durability performance of a driveshaft

Kardan mili dayanıklılığının tahmin edilmesi için bir yaklaşım

Onur ŞEN[1], Enver ATİK[2]*

[1]Tirsan Kardan A.Ş. R & D Center, Manisa, Türkiye.
firstauthor@e-mail.address, thirdauthor@e-mail.address
[2]Department of Mechanical Engineering, Faculty of Engineering, Manisa Celal Bayar University, Manisa, Türkiye.
fourthauthor@e-mail.address

Received/Geliş Tarihi: 16.11.2023 Revision/Düzeltme Tarihi: 04.03.2025 doi: 10.5505/pajes.2025.39129
Accepted/Kabul Tarihi: 07.03.2025 Research Article/Araştırma Makalesi

Abstract

In motor vehicles, driveshafts, which enable the power produced in the engine to be transmitted to the differential, are one of the major elements in the drivetrain. A driveshaft compensates for the angular and axial distance differences between the elements in the drivetrain, depending on road conditions while it provides rotation and power transmission. A driveshaft prototypes of frozen designs are manufactured to validate the product by subjecting it to laboratory and vehicle tests respectively. Laboratory tests are conducted via testing machine specially developed for driveshafts. Durability test, which is one of the laboratory tests to be conducted to determine the durability performance of a drive shaft in terms of the number of safe cycles for driveshaft, takes a long time causing the high cost. In this paper, an approach to estimate the durability performance of a driveshaft, using a new-developed analytical model, is presented. A new model has been developed that gives the number of safe cycles for the driveshaft as an output. The number of safe cycles here refers to the number of driveshaft revolution without any failure on the propeller shaft. The results from the new-developed model were compared with the durability test results of the driveshafts, it was seen that the results approached the test results with a difference of less than 5%. When the results obtained from the test and the model are considered, it is suggested to use the new-developed model instead of the durability test in determining the durability performance of the driveshaft.

Keywords: Driveshaft, Durability, Mathematical model, Laboratory test.

Öz

Motorlu taşıtlarda, motorda üretilen gücün diferansiyele iletilmesini sağlayan kardan milleri, aktarma organları içindeki en önemli elemanlarından biridir. Kardan mili, dönme hareketi ve güç aktarımını sağlarken, yol koşullarına bağlı olarak aktarma organlarındaki elemanlar arasındaki açısal ve eksenel mesafe farklarını da kompanse eder. Sırasıyla laboratuvar ve araç testlerine tabi tutarak doğrulamak için dondurulmuş tasarımların kardan mili prototipleri üretilir. Laboratuvar testleri, kardan milleri için özel olarak geliştirilmiş test cihazında gerçekleştirilmektedir. Bir kardan milinin emniyetli çevrim sayısı açısından dayanıklılık performansını belirlemek amacıyla yapılacak laboratuvar testlerinden biri olan dayanıklılık testi, uzun zaman aldığından yüksek maliyete neden olur. Bu makalede, yeni geliştirilen bir analitik model kullanılarak bir kardan milinin dayanıklılık performansını tahmin etmeye yönelik bir yaklaşım sunulmaktadır. Çıktı olarak kardan mili için güvenli çevrim sayısını veren yeni bir model geliştirilmiştir. Buradaki güvenli çevrim sayısı, kardan milinde herhangi bir arıza olmadan kardan milinin yaptığı devir sayısını ifade eder. Yeni geliştirilen modelden elde edilen sonuçlar, kardan millerinin dayanıklılık testi sonuçlarıyla karşılaştırılmış, sonuçların test sonuçlarına %5'in altında bir fark ile yaklaştığı görülmüştür. Test ve modelden elde edilen sonuçlar göz önüne alındığında kardan milinin dayanıklılık performansının belirlenmesinde, dayanıklılık testi yerine yeni geliştirilen modelinin kullanılması önerilmektedir.

Anahtar kelimeler: Kardan mili, Dayanıklılık, Matematik model, Laboratuvar testi.

Düzeltilmemiş Sürüm - Uncorrected Version

1 Introduction

Drive shafts are used to transmit the power generated in the engine from the motor or gear box to the rear or front wheels. They provide the connection between the transmission elements by compensating the angular and linear distance differences. When the motor vehicle is moving and loaded, the transmission elements displace as much as the suspension system allows. In both cases, the displacements occurring are compensated by the axial and angular movement of the propeller shaft. The angular movement capability of a driveshaft illustrated in Figure 1.1, is thanks to universal joints.

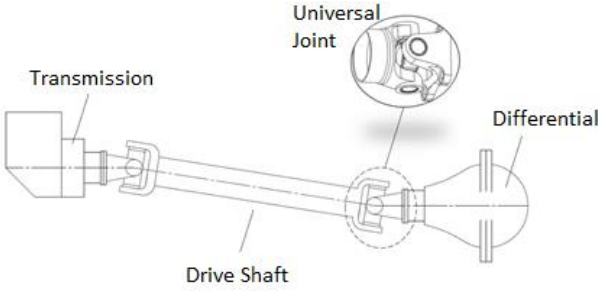

Figure 1.1. Universal joint and its angular position on the drive shaft.

A universal joint basically consists of two mutual parts with yoke geometry and a cross-shaft assembly providing a connection between two yoke parts as seen in Figure 1.2.

*Corresponding author/Yazışılan Yazar

Herkese Açık

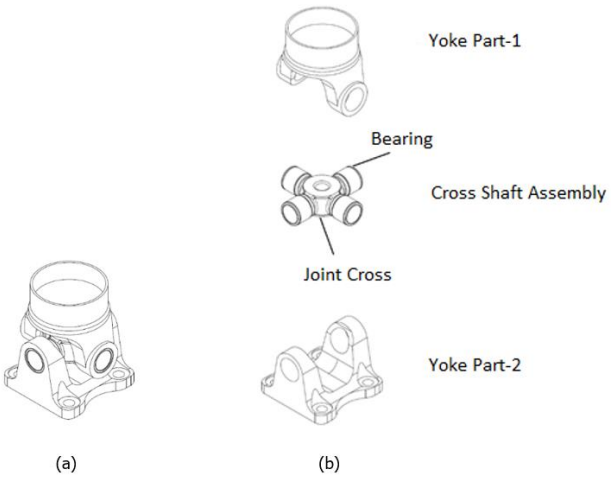

Figure 1.2. A typical universal joint: a) assembled view, b) exploded view.

A cross-shaft assembly simply involves a joint cross with four arms at the right angle to each other, and four closed-end needle roller bearings. The needle roller bearings are used to support the arms and to mount the arms into the yoke holes [1]. Needle roller is a kind of cylindrical roller having a highly small diameter compared to its length [2]. Although there are various rolling elements, needle rollers are used in the universal joint bearing. The main reason of why needle rollers are used in universal joints, is the cyclic loading resulting from the oscillating motion. Needle roller bearings have a line contact increasing the rigidity and maximum load capacity of the universal joint while the ball bearings have single point contact limiting the strength [3]. Additionally, considered that the inner volume of the bearing is narrow, needle roller is the one suitable rolling element for universal joints [4].

The fact that the bearing undergoes wear and ensures the transmission of torque between the two yoke parts makes the bearing the critical element that determines the durability performance of the driveshaft.

In most engineering applications, bearing selection and related engineering calculations are carried out according to the ISO 281:2007 [5] standard. The standard is based on the work implemented by Palmgren–Lundberg and Ioannides–Harris and expresses the basic service life prediction for radial rolling bearings (cylindrical, needle, barrel, and tapered roller) via Eq. (1.1) with 90% confidence. In the equation, ⍰r and ⍰r represent the radial load capacity and equivalent radial load on the bearing, respectively.

$$L_{10} = \left(\frac{C_r}{P_r}\right)^{10/3} \qquad (1.1)$$

When we investigated the study on life prediction carried out until today, many of which were included in the ISO standard, the beginning of the studies pointed to the 1800s. In these years, studies were started in the bearing industry to size bearings for specific applications and determine their life and reliability. Considering the significant studies carried out, it is seen that Stribeck [6] performed fatigue tests on bearings in 1896. In 1912, Goodman [7] introduced formulas based on fatigue data to calculate safe loads for cylindrical roller.

The most important improvement in life prediction about roller and ball bearings was made by Palmgren [8]. Using the Weibull distribution, Palmgren [9], [10], together with Lundberg, added a series of new studies to his work in 1945. And so, the outputs of this common study were included in the ISO 281:1990 [11] and ANSI/AFBMA-STD-9 [12] standards for calculating life and load capacity in rolling bearings.

Due to the emergence of different designs and material uses in roller bearings over time, the Lundberg Palmgren modification based on material fatigue limit and discrete finite elements was introduced by Ioannides and Harris [13] in 1985.

In the following years, Zaretsky [14] proposed a Weibull-based life theory in 1987, which considers deviations from the accepted Hertz stress-life relationship and uses the discrete finite element method. He adapted this theory to ball and roller bearings together with Poplawski and Peters in 1996 [15].

Modification studies based on fatigue limit and contamination for the Lundberg-Palmgren theory were carried on by other researchers in 1994-1995 [16]-[19]. In another study, a Lundberg-Palmgren based mathematical model was put forward by Tallian [20]-[22].

The said theories were summarized as the f(x) function in Table 1.1, so that they were compared with each other. Additionally, the statements that Zaretsky [23],[24] studied and revealed the relationship between these theories and life expectancy (L) were also included in the table.

Table 1.1. Life theories for roller bearings.

Life Theories	Functional Expression	Zaretsky's Perspective
Weibull (1939)	$f(x) = \sigma^e$	$L = A\left(\frac{1}{\tau}\right)^{\frac{c}{e}}\left(\frac{1}{V}\right)^{\frac{1}{e}} \sim \frac{1}{{S_{max}}^n}$ For line contact, n= 10.2 For point contact, n=11.1
Lundberg-Palmgren (1947-52)	$f(x) = \frac{\tau^c N^e}{Z^h}$	$L = A\left(\frac{1}{\tau}\right)^{\frac{c}{e}}\left(\frac{1}{V}\right)^{\frac{1}{e}}(Z)^{\frac{h}{e}} \sim \frac{1}{{S_{max}}^n}$ For line contact, n= 8.1 For point contact, n=11.1
Ioannides-Harris (1985)	$f(x) = \frac{(\tau - \tau_u)^c N^e}{Z^h}$	$L = A\left(\frac{1}{\tau - \tau_u}\right)^{\frac{c}{e}}\left(\frac{1}{V}\right)^{\frac{1}{e}}(Z)^{\frac{h}{e}} \sim \frac{1}{{S_{max}}^{n(\tau_u)}}$ For line contact, n= 8.1 For point contact, n=11.1
Zaretsky (1987)	$f(x) = \tau^{ce} N^e$	$L = A\left(\frac{1}{\tau}\right)^{c}\left(\frac{1}{V}\right)^{\frac{1}{e}} \sim \frac{1}{{S_{max}}^n}$ For line contact, n= 9.9 For point contact, n= 10.8

A : Material life factor	S_{max}: max. Hertzian stress (GPa)
c : Critical shear stress-life exponent	V : Volume under stress (m3)
e : Weibull slope	Z : Distance to critical shear stress (m)
f(x): life function	σ : Stress (GPa)
h : exponential constant	τ : Critical shear stress (GPa)
L : Life, number of cycles	τ_u : Fatigue limit (GPa)
N : Number of stress cycles causing damage	c/e : Stress-life exponent
n : max. Hertz stress-life exponent	

It was mentioned that the studies on bearing life prediction were based on Hertz's work. Therefore, these studies include the Hertz stress-life exponent (n). The value of Hertz stress-life exponent varies between approaches. And so, the value of the load-life exponent (p) also varies. The values of the load life

Düzenleme Kurulu Sürüm - Unformatted Version

Herkese Açık

exponent according to the approaches were calculated and compared in Table 1.2.

Table 2.2. Hertz stress-life and load-life exponent for linear contact.

Life Theories	Hertz stress-life exponent, n	Load-life exponent, p
Weibull (1939, 1964)	$n = \frac{c+1}{e}$ (e=1.11; c/e= 9.3; h=2.33)	p=n/2 (p=5.10)
Lundberg-Palmgren (1947)	$n = \frac{c+1-h}{e}$ (e=1.11; c/e= 9.3; h=2.33)	p=n/2 (p=4.05)
Ioannides-Harris (1985)	$n = \frac{c+1-h}{e}$ (e=1.11; c/e= 9.3; h=2.33)	p=n/2 (p=4.05)
Zaretsky (1987)	$n = c + \frac{1}{e}$ (c=9; e=1.11)	p=n/2 (p=4.95)

For Lundberg-Palmgren [9], the load-life exponent p should be 4 for the linear contact case (p=4, n=8.1 for 2.4 GPa max Hertz stress and 1.11 Weibull slope). Although this value was later suggested as 10/3 by Lundberg-Palmgren [10] (1952), in the studies carried out by Zaretsky et al. [15] in 1996, it was found more consistent to take the load-life exponent as 4. On the other hand, rolling elements made of steel produced under vacuum, such as AISI 52100, exhibited a load-life exponent of 5 for cylindrical rolling elements and 4 for ball elements. Because the inclusions in the bearing steel do not harden because of the vacuum process, the material offers a longer life compared to melting in air (air melted/AM) [25].

When we examine the equations in Table 1.1, when there is no specific fatigue limit in the Ioannides Harris equation (u = 0), it becomes equivalent to the Lundberg-Palmgren method. Weibull analysis also approaches the Zaretsky method if the same exponential constant selection is made, as expressed in

$$L_{10} = \left(\frac{C}{P}\right)^{p} \quad (1.2)$$

C, P and p are the dynamic load capacity of the bearing, the equivalent radial load on the bearing and the load-life exponent, respectively. The load-life exponent p is taken as n/2 for the linear contact case.

ISO/ANSI standards take the load-life exponent (p) as 10/3 for the linear contact case. Thus, the Hertz stress-life exponent (n) takes the value of 6.6 (for 2.4 GPa max Hertz stress and 1.11 Weibull slope), which results in the calculation of lifetimes lower than the actual situation in the field [23]. On the other hand, it should not be forgotten that in the studies carried out by Zaretsky et al. [15], taking the load-life exponent as 4 was found to be more consistent.

It was observed that both methods developed by Ioannides and Harris and Zaretsky were compatible with each other, while the Lundberg-Palmgren method differed and remained on the safe side.

Service life predictions for rolling bearings were presented with different approaches in the literature, as mentioned above. However, these approaches consider rolling bearings individually and require new experimental studies to predict the service life of mechanical elements such as driveshafts. Therefore, this study aimed developing a new analytical model based on the bearing used in the joint, which predicts the number of safe cycles referring to number of the driveshaft revolution without any fault on the driveshaft. The outputs from the new-developed model were obtained as the number of safe cycles and were compared with each other besides the laboratory test results of the driveshafts.

2 Methodology

The studies were carried out in two different methods: laboratory tests and analytical studies. Laboratory tests involve physically testing the driveshaft samples in the laboratory condition while analytical studies include the development of a new mathematical model predicting the number of safe cycles

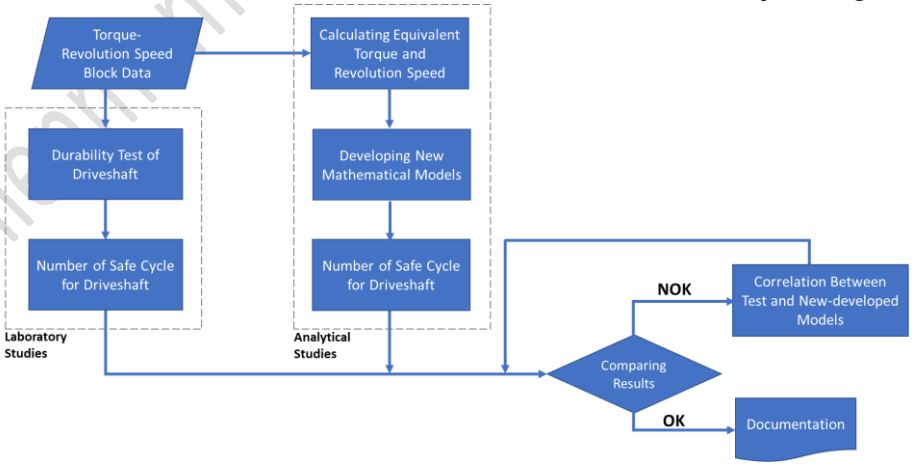

Figure 2.1. The road map of the methodology followed in the study.

Table 1.2. From the Lundberg-Palmgren [9] equation, the bearing life L10 with 90% reliability, expressed in million cycles, is determined by the Eq. (1.2).

which refers to number of the driveshaft revolution without any fault on the driveshaft. Laboratory and analytical studies were conducted on the driveshaft used on light commercial

Düzenlenmiş Sürüm - Uncorrected Version

Herkese Açık

vehicles with the following technical characteristics given in Table 2.1.

Table 2.1. Technical characteristics for the driveshaft.

Connection type	SAE connection
Joint bearing size	Ø27 x 25
Angle compensation	15°
Length compensation	max. 84 mm
Driveshaft length	1000 ±2 mm

The studies are carried out by following the road map given in Figure 2.1. In both the analytical studies and laboratory tests, the torque-speed block data of the sample driveshaft was used as input. While the results of the laboratory test were recorded, number of safe cycles was predicted using the new-developed mathematical model. The results obtained from both methods were compared with each other.

2.1 Development of a new mathematical model

In the analytical studies, developing a new mathematical model predicting the number of safe cycles of driveshaft was aimed. The new-developed mathematical model is based on considering the variable load, which is created by the torque transferred to the driveshaft, on the cross-shaft assembly through the universal joint and finally on the bearing.

In the durability test carried out under laboratory studies, the driveshaft will perform its function until the driveshaft cross-shaft assembly under load is damaged and will reach a certain number of cycles, which is called the number of safe cycles, during this period. The new-developed mathematical model considers parameters such as fatigue load limit (□u), load-life exponential (P), dynamic load capacity of the bearing (Cr), affecting the crack propagation process, which starts from the surface fatigue crack on the surface of the bearing elements and progresses to the critical crack length, leading to pitting.

The activities followed in developing mathematical model were detailed in Figure 2.2.

In the studies, firstly, equivalent values for torque and rotational speed were calculated based on the block data of the sample driveshaft. The obtained values were used to calculate the radial load on the bearing. The radial load was reduced to the unit load on the rolling elements that compose the bearing, and the next step was to reveal the effect of Hertz pressure on the elements. It was checked whether it was on the safe side by comparing the calculated Hertz pressure with the safe contact pressure value (4000 MPa for roller bearings) specified in the ISO 76 1997 [26] standard and determined by taking different experimental studies as reference. By making sure that the pressure remained on the safe side, static strength was checked and the calculation of the estimated bearing life, which is the last step of the mathematical model study, was used to obtain the number of cycles of the driveshaft until the bearing damage. The study presented in this order was conducted in the light of the following assumptions:

- Losses that may occur because of friction in the universal joints during the movement of the driveshaft have been neglected.

- Possible gaps that may occur over time in the connection pairs (flange and bolt) used in the driveshaft assembly have been neglected.

- It is assumed that the driveshaft joint bearings did not lose grease during the test. For this purpose, during the tests, the testing machine was stopped from time to time for short periods, and the bearing sealing were checked for possible grease leaks. As a result, no leakage was found on any driveshaft samples.

2.1.1 Calculation of equivalent values of torque and revolution speed

Driveshafts don't operate at maximum torque values continuously. If the driveshaft for a vehicle is selected by considering the maximum torque value, an over-designed driveshaft will be used, which will increase its cost and weight. Therefore, driveshaft data is collected from real road conditions and then turned into a block. Driveshaft laboratory tests are conducted by using this data set also known as block data.

Equivalent torque and revolution speed values can be calculated by means of Eq. (2.1) and Eq. (2.2), respectively, by using block data consisting of time-varying torque and speed data, an example of which is given in Table 2.2 [27].

Table 2.2. Block data structure for a driveshaft.

Torque (Nm)	Revolution speed (rpm)	Time rate (%)
T_1	n_1	q_1
T_2	n_2	q_2
...	...	...
T_i	n_i	q_i

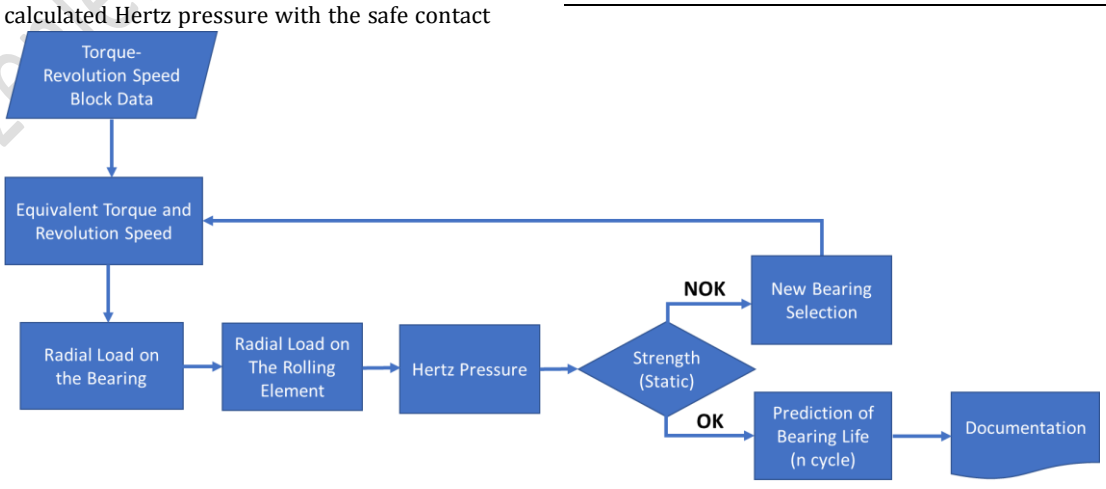

Figure 2.2. Detailed flow diagram for the mathematical model study.

Düzeltilmemiş Sürüm - Uncorrected Version

Herkese Açık

$$T_e = \sqrt[3]{\frac{T_1^3 . n_1 . q_1 + \cdots + T_i^3 . n_i . q_i}{n_1 . q_1 + \cdots + n_i . q_i}} \quad (2.1)$$

$$n_e = \frac{n_1 . q_1 + \cdots + n_i . q_i}{q_1 + \cdots + q_i} \quad (2.2)$$

In the equations, Te and ne express the equivalent torque and revolution speed, respectively; Where i is the row number, Ti, ni and qi represent the percentage weight in terms of torque, revolution speed and time, respectively.

In the study, block data shared as Table 2.3. was used as input, and the equivalent torque and revolution speed values, which were calculated by using Eq. (2.1) and Eq. (2.2), were given in Table 2.4.

Table 2.3. Driveshaft block data used in the studies.

Torque (Nm)	Revolution speed (rpm)	Time rate (%)
925	1348	0.7
1125	1645	1.5
...	...	...
...	...	...
300	554	13.4
350	880	10.6

Table 2.4. Equivalent torque and revolution speed values calculated from block data.

T_e (Equivalent torque)	660.04 Nm
n_e (Equivalent revolution speed)	1499.83 rpm

2.1.2 Oscillation angle on joint

The rolling elements on a universal joint bearing follow the path illustrated in Figure 2.3 for one revolution of the driveshaft. The points marked 0 and 4 on the figure indicate the first and last positions of a rolling element, respectively. The angle of the path followed between two points (for example 2 and 3) is expressed as the oscillation angle. The oscillation angle Ø is defined by Harris and Kotzalas [28], [29] as 1/4 of the total arc followed by the rolling element during one rotation of the driveshaft.

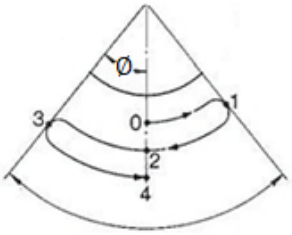

Figure 2.3. The oscillatory motion of a rolling element for one revolution of the joint.

To determine the oscillation angle, a three-dimensional joint model was run using the Motion interface of SolidWorks software. In the simulation, it was determined that the oscillation angle drawn in each movement (¼ turn) was equal to the operating angle of the driveshaft joint. An example simulation expressing this situation, run for a 7° joint angle, was given in Figure 2.4.

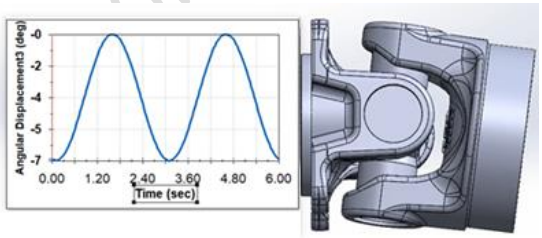

Figure 2.4. A simulation example to determine the oscillation angle for a 7° joint angle.

2.1.3 Determination of radial load on the bearing

In this section, the bearing, which is subjected to load with the effect of the torque carried by the driveshaft, was examined and the radial load acting on the rolling elements was also calculated.

While the dimensional properties of the joint cross under load are given in Figure 2.5, the basic dimensions of the bearing and trunnion on the yoked part are given in Figure 2.6. In the figure, the radial loads under the influence of the forked part and thus the bearing are expressed

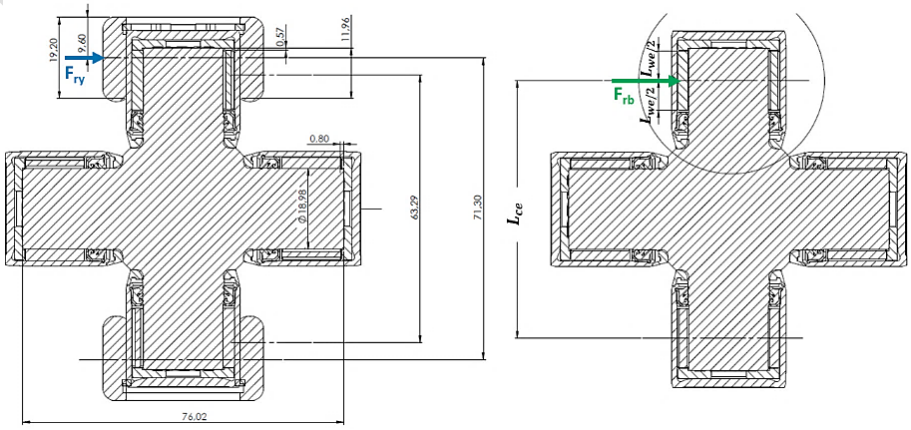

Figure 2.5. Joint cross with its geometry and dimensional properties.

Düzenlenmemiş Sürüm - Accepted Version

Herkese Açık

as Fry and Frb, respectively.

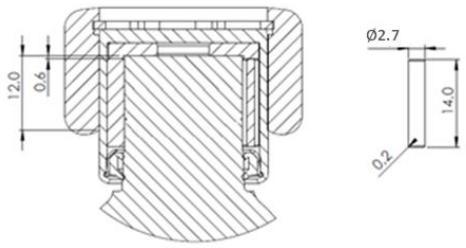

Figure 2.6. Basic dimensions for the bearing and trunnion on the yoked part.

The maximum radial load on the bearing occurs as Frb when the driveshaft rotates by 90°. Based on this, the loads acting on the output trunnion of the driveshaft for the 8° and 11° joint angles, where laboratory tests were carried out, were calculated by means of Eq. (2.3).

$$F_{rb} = \frac{T_2}{L_{ce}} \tag{2.3}$$

In the equation, Frb, T2 and Lce express the radial load on the output arm of the joint cross, the output torque value and the effective length of joint cross arm, respectively. Here, T2 was calculated with Eq. (2.4) where ▯▯ and ▯▯ refer to the torque values at the input and output yoke, respectively, ▯ refers to the joint angle, and ▯▯ and ▯▯ refer to the rotation angle of the input and output yokes, respectively. Lce value was be calculated by using the Eq. (2.5) and Eq. (2.6) respectively.

$$T_2 = T_1 \frac{\cos^2 \varphi_1 \cos^2 \beta + \sin^2 \varphi_1}{\cos \beta} \tag{2.4}$$

$$L_{we} = L_s - h_s - (2\,i - 1)\, r_w - (i - 1)\, t_w \tag{2.5}$$

$$L_{ce} = L_c - 2h_s - 2L_{we} - (2\,i - 2)\, r_w - (i - 1)\, t_w \tag{2.6}$$

Among the parameters in the equations above, Lwe is the effective roller length, Ls is the supported trunnion length, hs is the interface length between the trunnion and roller surfaces, i is the row of rollers in the bearing, rw is the roller end radius value, tw is the thickness of the washer separating the rows in two-row bearings, and finally Lc represents the joint cross arm length. The values of these parameters were taken from Figure 2.5 and Figure 2.6 for the joint cross used in the tests.

Finally, for 8° and 11° joint angles, T2, Lce and Frb are calculated and expressed in Table 2.5.

Table 2.5. Calculated values for joint angles 8° and 11° for 90° rotation of the driveshaft: T2, Lce and Frb.

Joint angle β	Output torque value (T_2)	Effective length of joint cross arm (L_{ce})	Radial load on the output arm of the joint cross (F_{rb})
8°	666.49 Nm	63.69 mm	10464.53 N
11°	672.35 Nm	63.69 mm	10556.65 N

2.1.4 Determination of radial load on the rolling Element

The load acting on the bearing is distributed on the rollers depending on the position of the rollers. Roller numbered 1, which makes an angle of 0° with the radial load shown in Figure 2.7, carries the highest load. In other rollers, considering that the radial load divides the bearing into two equal parts, the rollers arranged on the right and left sides of the roller numbered 1 form a pair, and the rollers forming each pair carry the same load as each other.

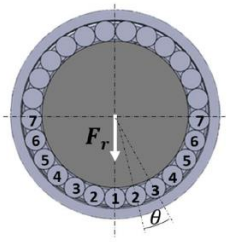

Figure 2.7. Rollers under loading condition.

The loads on the rollers were calculated for 8° and 11° joint angles using the equations given in Table 2.6. The load values obtained for each rolling element are given in the same table.

Table 2.6. At 8° and 11° joint angles, load on the rolling elements distribution (Qi).

Symbol	Equation Used	Results	
		β =8°	β =11°
$J_r(\varepsilon)$	2.8	0.245	0.245
$Q_1 = Q_{max}$	2.7	1708.50 N	1723.54 N
Q_2	2.9	1648.96 N	1663.48 N
Q_3		1475.36 N	1488.35 N
Q_4		1202.45 N	1213.04 N
Q_5		854.14 N	861.66 N
Q_6		463.37 N	467.45 N
Q_7		78.88 N	79.57 N

$$F_{rb} = Q_{max}\, z\, J_r(\varepsilon) \tag{2.7}$$

$$J_r(\varepsilon) = \frac{1}{2\pi} \int_{-\psi_1}^{+\psi_1} \left[1 - \frac{1}{2\varepsilon}(1 - \cos\psi)\right]^m \cos\psi\, d\psi \tag{2.8}$$

$$Q_i = Q_1\{\cos[(i-1)\theta]\}^m \tag{2.9}$$

On the Eq. (2.7) and Eq. (2.8) developed by Stribeck [30]-[31], ▯, z, ψ, ▯, and ▯ (ε) are respectively the radial load on the bearing, the number of rollers in a single row, the position angle of the rolling element, the maximum radial load on the roller at a position angle of 0°, and the radial load integral. Another parameter m represents an exponential constant and is taken as 1.11 for roller bearings and 1.5 for ball bearings [6],[32].

On the Eq. (2.9), ▯ represents the angle between the adjacent rollers, i takes the value 2, 3, 4, ..., n+1, and the exponential constant m takes the value 10/9 for linear contact and 3/2 for point contact [33].

Düzeltilmemiş Sürüm - Uncorrected Version

Herkese Açık

2.1.5 Determination of contact pressure

In this section, the Hertz contact pressure on the rollers under load at the moment it has the highest load was calculated and compared with the safe pressure value of 4000 MPa defined in the ISO 76:1997 [26] standard. For this purpose, contact pressures were calculated for 8° and 11° joint angles using following equations.

If the distribution of contact pressure along the x-axis (as in Figure 2.8) is examined, the contact pressure P(x), which varies depending on the position on the x-axis, can be calculated by means of Eq. (2.10) [34].

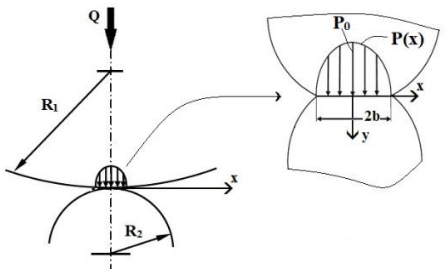

Figure 2.8. Contact pressure distribution between two cylindrical elements.

$$P(x) = \frac{2\,Q}{\pi\,L_a\,b^2}\sqrt{b^2 - x^2} \qquad (1.10)$$

Here, Q is the radial load on a roller, La (2l) is the contact length, x is the distance of the contact pressure from the origin, and b is half the contact width. Eq. (2.11) can be used to calculate half of the contact width (b).

$$b = \sqrt{\frac{4\,Q\,R^*}{\pi\,L_a\,E^*}} \qquad (2.11)$$

On the equation, R* represents the relative radius of curvature and E* represents the equivalent elasticity modulus. These parameters can be calculated using the Eq. (2.12) and Eq. (2.13) where R is the radius of curvature and E is the equivalent elasticity modulus. In the symbols, while number 1 indicates the first contact element, number 2 indicates the second contact element.

$$\frac{1}{E^*} = \frac{1 - {v_1}^2}{E_1} + \frac{1 - {v_2}^2}{E_2} \qquad (2.12)$$

$$\frac{1}{R^*} = \frac{1}{R_1} \pm \frac{1}{R_2} \qquad (2.13)$$

The contact pressure on the rolling element reaches its highest value at the contact center, in other words, at the axis of the radial load (x=0), while it tends to decrease as it moves away from the axis (x≠0). When the joint angle is examined, the load on the bearing increases depending on the increasing joint angle, and therefore the contact pressure on the rolling element increases. And so, the highest contact pressures were calculated as 1392.62 MPa and 1398.74 MPa respectively for joint angle 8° and 11°. Both were on the safe side by not exceeding the 4000 MPa threshold. Therefore, the next step was started. In other words, the number of safe cycles was predicted for the driveshaft operating at 8° and 11° joint angles.

2.1.6 Determination of dynamic load capacity of bearing

In this section, the load that the bearing can dynamically carry was determined to be used in predicting the number of safe cycles. The Cr value for the bearing was calculated using the dynamic load capacity equation for radial bearings, Eq. (2.14).

$$C_r = b_m\,f_c\,(i\,L_{we}\cos\alpha)^{7/9}\;z^{3/4}\;{D_{we}}^{29/27} \qquad (2.14)$$

On the equation, bm and fc are the rating factors, i is the number of rows in the roller arrangement, z is the number of rollers in a row, Lwe is the effective length of the roller, α is the nominal contact angle, Dwe is the cross-sectional diameter of a roller.

Values of rating factors bm and fc were respectively taken as 1.10 and 86.77 by using the table in ISO 281:2007 [5]. Rating factor bm and fc are selected from the related table depending on the bearing type, roller diameter, trunnion diameter and nominal contact angle.

All the parameters needed in Eq. (2.14) to calculate the dynamic load capacity (Cr) were determined and the Cr value was calculated as 20452.9 N. Table 2.7 shows the calculated Cr and the values of the parameters used in its calculation.

Table 2.7. Calculated dynamic load number and values of the parameters used in its calculation.

L_{we} (mm)	D_{we} (mm)	D_t (mm)	z (pcs)	i (pcs)	f_c	b_m	C_r (N)
11.19	2.72	18,9	25	1	86.8	1.1	20452.9

2.1.7 Predicting the number of safe cycles of the drive shaft

Since the use of numerical methods requires a long study involving modeling and definition of boundary conditions, analytical methods can be preferred. In this context, a fundamental solution for frictionless elastic contact on bearings was found by Hertz in 1882 [35], and several studies on Hertz's solution were presented by including different contact situations [36]-[38].

In this section, which is the last step of the mathematical model study road map, all the steps followed up to this point have been combined and used in the mathematical model study that gives the safe number of cycles for the driveshaft, considering the literature studies.

In the model, Oscillatory movement, which has a great effect on the rolling elements of the propeller shaft, has been adapted to the model. as given in Table 2.8.

The load-life exponent (p), which has another critical effect, was taken as 4.95 in the studies carried out by Zaretsky [14], while it was taken as 4.05 in the studies of Lundberg-Palmgren [9] and Ioannides-Harris [13]. In order to approximate the results of the driveshaft tests, both different values were taken into consideration. As a result, the load-life exponent value was taken as 4.05 and the model achieved successful results.

The new-developed model was called as Model-SA so that they could be remembered easily.

Düzenlenmiş Sürüm - Uncorrected Version

Herkese Açık

Table 2.8 New-developed mathematical model: Model-SA

Model-SA	$L_{osc,10} = \left(\frac{C_r}{P_{osc}}\right)^p f_m$	(2.15)
Oscillation effect	$P_{osc} = F_{rb}\left(\frac{2\,\emptyset}{180°}\right)^{1/p}$	(2.16)
Modification factor	$f_m = 0.1\left[1-\left(2.5671-\frac{1.9987}{K^{0.071739}}\right)^{0.83}\left(\frac{e_c c_u}{F_{rb}}\right)^{1/3}\right]^{-9.3}$	(2.17)

In the above equations for the new-developed model;

L_{osc10}: It expresses the number of safe cycles of driveshaft which refers to number of the driveshaft revolution without any fault on the driveshaft.

C_r: It expresses the dynamic load capacity of the bearing and is calculated with Eq. (2.14). The dynamic load capacity calculated for the bearing used in the tests is given in Table 2.7.

P_{osc}: It symbolizes the equivalent radial load on the bearing in the joint under oscillatory movement and is calculated with Eq. (2.16). In the equation, Frb refers to the radial load on the bearing, Ø is the oscillation angle and p is the load-life exponent.

P: It is the load-life exponential constant and is used as 4,05.

f_m: It symbolizes the modification factor. It is calculated with the corresponding Eq. (2.17) in ISO 281:2007 [5].

C_u is the fatigue load limit and is calculated with Eq. (2.18) below.

$$C_u = \frac{C_0}{8{,}2} \qquad (2.18)$$

e_c is the contamination factor and it was taken as 1 because the experimental studies were carried out in a laboratory environment.

F_{rb} is the equivalent load on the bearing.

κ viscosity ratio varies depending on the characteristics of the grease used in the bearing and is calculated according to ISO 281:2007 [5].

2.2 Laboratory studies on durability tests of driveshaft samples

Durability testing machine for the laboratory studies, which were taken as reference for the verification of the new-developed model and a driveshaft sample used in tests were shown in Figure 2.9. The testing machine uses a specific torque and speed values as test input. The testing machine allows four driveshaft samples to be tested at the same time at a certain working angle thanks to its middle unit.

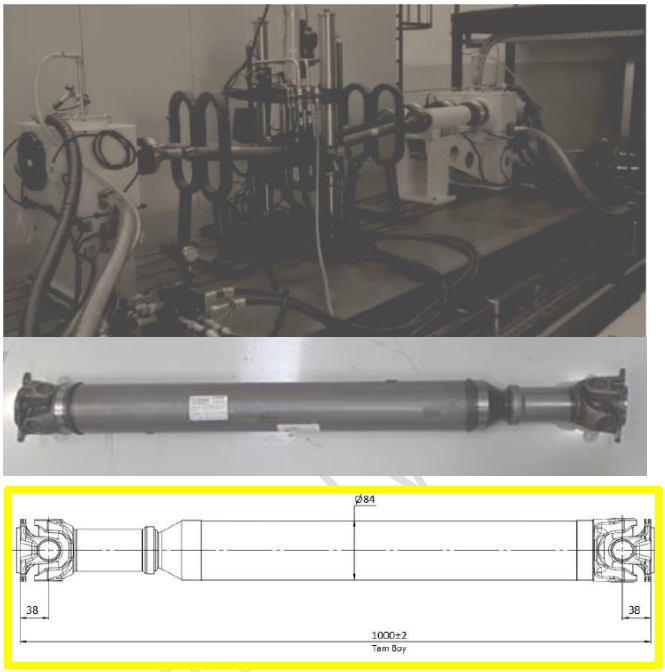

Figure 2.9. Durability testing machine and a driveshaft sample.

Firstly, four samples of the driveshaft which were selected to be used in the calculations by new developed mathematical model, were fixed on the testing machine. After that, an infrared (IR) sensor per a universal joint was placed in such a way that they could track the bearing surfaces to measure the temperature, which is generated due to the friction, on the bearings of the universal joints as expressed in Figure 2.10. IR sensors were numbered and connected to the data acquisition (DAQ) device collecting temperature data. The type of temperature sensor was selected depending on the frequency of data collection, the temperature range to be measured and the method of data collection (wired or wireless). The view of the IR sensor and its specifications were shared in Figure 2.10.

Measurement range	Sensitivity	Reaction time	Accuracy
-50 °C +600 °C	0,1 °C	150 ms (%95)	±1 %

Figure 2.10. IR sensor: location on the test machine, its specifications.

The tests were carried out at the values shared in Table 2.3 to compare with the numbers of safe cycles which were calculated for 8° and 11° joint angles by using the new-developed model.

It is worth remembering that the drive torque and rotational speed, which is defined in Table 2.9, were calculated as equivalent values from the block data. Safe cycle predictions were calculated by considering these equivalent values and using new-developed model.

Düzeltmeli Sürüm - Turkish

Herkese Açık

Table 2.9. Inputs to testing machine in laboratory tests.

Joint angle	Driven torque	Revolution speed
8° 11°	660.04 Nm	1499.83 rpm

During the operation of the driveshaft, the temperature increase that occurs in the bearings over time. In other words, the trend change in temperature, is a factor that indicates the disruption of the driveshaft, after which point the loss of function in the driveshaft begins. Based on this phenomenon, in the durability tests of the driveshaft, the temperature trend developing for each bearing, was monitored instantly by means of IR sensors.

During the tests, the test was stopped for a short time to check whether there was any oil leakage in the bearings and continued by making sure that there was no leakage (this process appears in the temperature graphs as a temperature of zero value for a moment).

Otherwise, possible grease loss in the bearings may mislead by affecting the number of safe cycles. When a sudden change in the temperature trend was detected, the test was terminated, and the number of cycles of test samples was recorded. The change in temperature trend alone, which is a symptom of damage to the joint cross and bearing, is not sufficient. For this reason, the joints of the driveshafts were subsequently disassembled into unit parts to be examined for damage. During examination, the detected damages were rated according to the colour chart specified in Table 2.10.

Table 2.10. Bearing failure rating table.

	Totally Damaged No surface area undamaged
	Surface-Wide Damage Spalling or Brinelling
	Localized Damage Spalling or Brinelling
	No Damage, No Spalling (pitting) or Brinelling Discoloration or markings
	No Damage, No Mark Shining

The definitions of the driveshaft samples and temperature sensors used in the tests are given in Table 2.11. As seen on the table, the tests were grouped under two separate headings as Group-I and Group-II, as they were carried out at different times for comparison with mathematical modelling studies. In the table, the layout of the driveshafts on the testing machine was given as well. The definitions A, B, C and D indicates different shaft on the testing machine. Symbol Ti (i=1, 2, ..., 8) defines the IR sensors used for each joint. And finally, driveshaft samples were tested under the conditions defined on Table 2.2 and Table 2.3.

Table 2.11. Overview to laboratory tests.

Test Group	Angle	Shaft Number	Sample Quantity
Group I	8°	1 2	2
	11°	3 4	2
Group II	8°	5 6	2
	11°	7 8	2

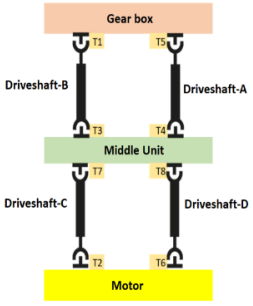

3 Results

During the laboratory tests, when the sudden change in temperature observed with IR sensors occurred, the test was stopped, and data was collected to be compared with the mathematical model as given in Figure 3.1 and Figure 3.2. The figures show the temperature values corresponding to the time elapsed in the test. The cycle time was calculated from the time elapsed when the test was stopped. After stopping the test, the driveshafts were disassembled and the bearings were examined and evaluated for the damage by rating according to the rating chart in Table 2.10. To make the evaluation of the bearing more understandable, the failure rating of some damaged bearings was shared in Table 3.1.

It can be said that at least one trunnion-bearing pair in each joint examined falls into the orange color zone and there is no contact pair falling into the red zone. This indicates that the damage caused by the increase in the temperature trend can be used in mathematical model calculations. Thus, it was determined that the driveshafts can be used in the correlation study between mathematical model and laboratory tests.

Table 3.1. Examples for evaluation of the bearings.

	X	• Partial spalling and partial brinelling were observed. • Local color change was observed, but not intense.
	X	Spalling mode was observed in narrow area.

The results of new-developed mathematical model and laboratory tests were compared with each other. Since the aim

Düzenlenmemiş Sürüm - Uncorrected Version

Herkese Açık

of the study is to predict the life of the cross bearing and so the number of safe cycles of the driveshaft by using a new-developed mathematical model instead of physical tests, the test results were taken as reference in comparing the mathematical model. In general, the acceptable level of percentage difference varies depending on the nature of the measurement. For example, if there is a difficult measurement, 10% is an acceptable level, while a measurement difference of 1% is very difficult to achieve [39]. In this study, the acceptable percentage difference between the results obtained by experimental and mathematical methods was targeted at 5% at most and the results were evaluated.

The percentage difference of the prediction made with the new-developed mathematical model, according to the test results, were revealed using Eq. (3.1) for 8° and 11° joint angles, and the results are shared in Table 3.2.

$$E_p = \frac{L_t - L_m}{L_t} 100 \qquad (3.1)$$

In Equation, Ep, Lt and Lm are the percentage difference, the life obtained by the test and the life obtained by the mathematical model, respectively.

In order to reveal the closeness of Model-SA to the test results compared to the existing approaches in the literature, the life values for 8° and 11° joint angles with the existing approaches and their percentage differences compared to Group-I tests are also calculated and given in Table 3.3.

When the percentage differences in Table 3.3 are examined, it is seen that the closest results to the test results are obtained by Zaretsky and Weibull approaches for the 11° joint angle, with 1.96% and 8.27%, respectively. On the other hand, it is found that neither of these approaches can approach the test results for the 8° joint angle. This shows the limitation of approaches by Zaretsky and Weibull.

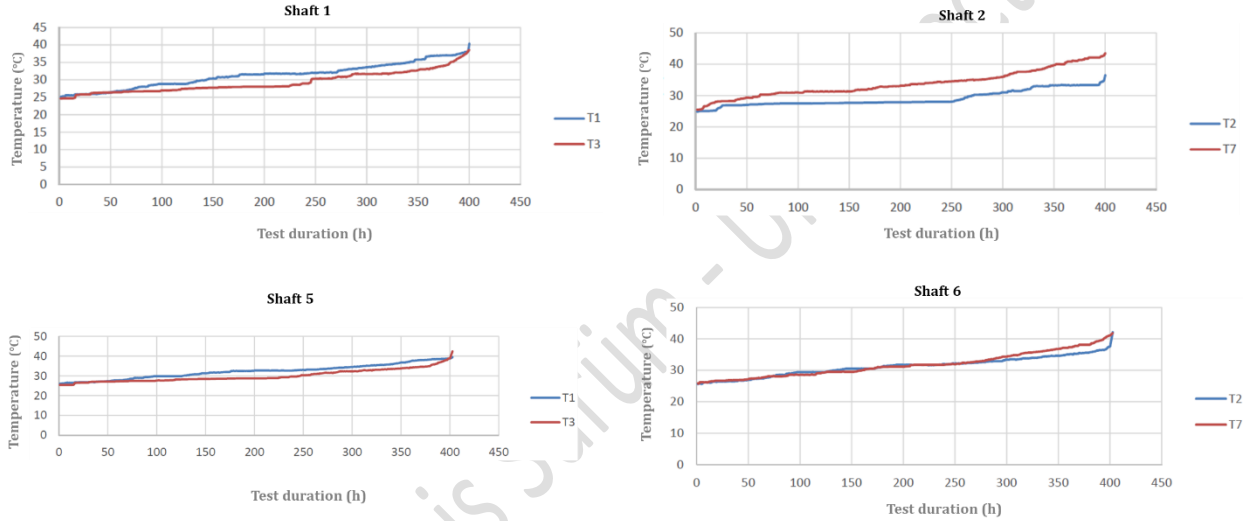

Figure 3.1. Temperature change in driveshafts tested at 8° joint angle (Shaft 1, 2, 5 and 6)

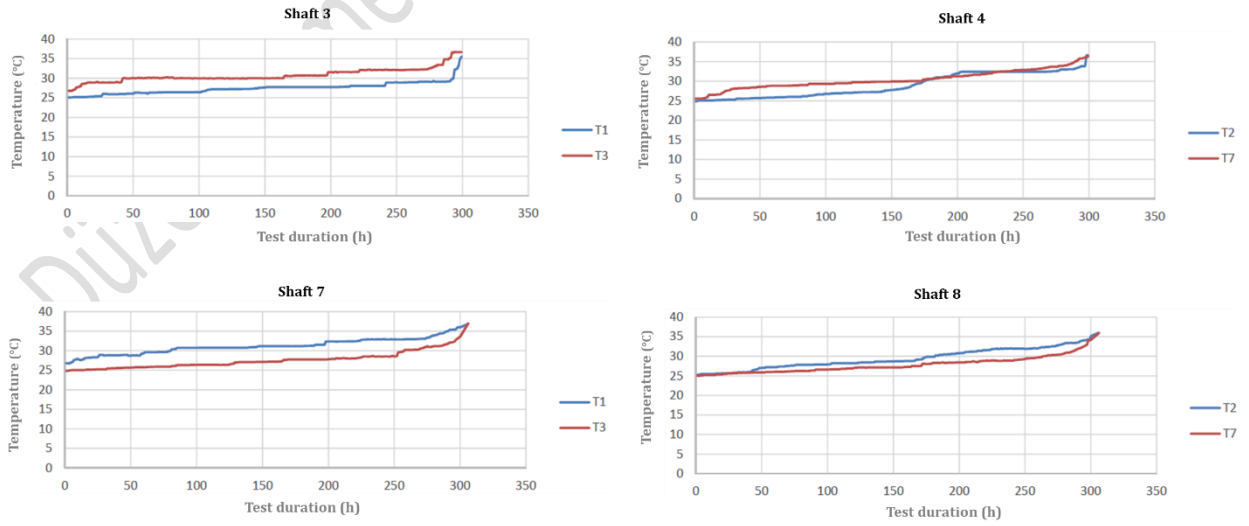

Figure 3.2. Temperature change in driveshafts tested at 11° joint angle (Shafts 3, 4, 7 and 8)

Herkese Açık

Table 3.2. Percentage difference for Model-SA.

	8° Joint angle			11° Joint angle		
	Test	Model-SA	Percentage difference	Test	Model-SA	Percentage difference
Test Group I	399.975 h	419.354 h	%4.84	299.351 h	306.687 h	%2.45
Test Group II	402.506 h		%4.19	306.109 h		%0.19

Table 3.3. Percentage differences in terms of Group-I Test results between Model-SA and approaches in literature.

Existing Approaches and Model-SA	Results for 8° joint angle			Results for 11° joint angle		
	by current approaches	Test	% Difference	by current approaches	Test	% Difference
ISO 281	103.50 h	399.975 h	-74.12	100.53 h	299.351 h	-66.42
Weibull	338.91 h		-15.27	324.09 h		8.27
Zaretsky	306.50 h		-23.37	293.49 h		-1.96*
Ioannides-Harris	167.69 h		-58.08	161.84 h		-45.94
Lundberg-Palmgren	167.69 h		-58.08	161.84 h		-45.94
Model-SA	419.35 h		**4.84***	306.68 h		**2.45***

***** Error rates below 5% are indicated in bold characters.

4 Conclusion

Cross-shaft and bearings in driveshafts are under the influence of oscillatory motion, which is of critical importance in mechanical systems. Therefore, joints are vital in determining the service life of the driveshaft. Durability tests is a major test used for determining service life of driveshaft. As can be expected, it takes a long time for the tests to be completed. Based on this, in the study initiated, the change in driveshaft service life for 8° and 11° joint angles was observed and a new mathematical model was developed as an alternative to the durability tests carried out in the laboratory environment. Laboratory tests (durability test) were carried out for 8° and 11° joint angles on the driveshaft samples produced for this purpose. On the other hand, existing approaches in the literature were compared both among themselves and with the new-developed mathematical model in terms of closeness to test results.

Both the test results and the mathematical model indicated that when the torque and revolution speed transmitted to a driveshaft are constant, the increase in the joint angle has a reducing effect on the service life of the driveshaft. For this reason, although the location and number of underbody components affect the layout of the driveshaft, the driveshafts should be placed to see the least possible joint angle under the vehicle. In addition, considering that road conditions affect the driveshaft joint angle, the road conditions (highway, construction site, city, etc.) and at what rate the vehicle operates become important for the driveshaft life expectancy.

It was determined that the service life predictions calculated using the approaches available in the literature were far from the test results. Here, although Zaretsky's model, one of the existing approaches, gave an error rate of less than 5% for an 11° joint angle compared to other existing approaches, the error rate reached 23.37% for an 8° joint angle. For this reason, Zaretsky's model, which came closest to the test results, was not recommended to be used instead of durability tests to determine the life of the driveshaft.

Due to the oscillatory movement that occurs due to the structure of the driveshaft joint, the load on the trunnion and roller does not remain constant and reaches different values for each rotation of the driveshaft. For this reason, it was seen in mathematical model development studies that the estimated life value calculated by taking the oscillation effect into consideration increased.

Considering that the results obtained with the new-developed mathematical model Model-SA is close to the test results with a difference of 4.84% and are closer to the test results than existing approaches, it is recommended to use this model as an alternative to durability tests to predict the life of the driveshaft. Additionally, as an extension of the study presented, the tests performed can be repeated using the Taguchi experimental design method.

The life of the driveshaft can be predicted within minutes with error rates below 5% by using the new-developed mathematical model Model-SA. And so, savings in energy, maintenance and man-hour costs can be achieved by reducing or resetting the number of durability tests.

According to the comparison study conducted on the contact models in the literature on the cylindrical element pair example, it has been determined that the Johnson, Radzimovsky and Pereira's models can be used interchangeably when both low and high loads are involved. Goldsmith's model can be used for low loads, while Lankarani and Nikravesh's model can be used for large loads. The new-developed mathematical model Model-SA has been validated with low loads for the driveshaft. However, considering that the said model was developed specifically for the driveshaft, making a comparison with the approaches in the literature in terms of the size of the loads may be misleading. The Hertz's model, which is seen as the ancestor of contact models, remains far away from all other models when it comes to high loads.

Düzeltmeler Sonrası - Uncorrected Version

Herkese Açık

However, when very low loads are involved, it can come close to other modelling.

5 Acknowledgment

6 Author contribution statements

In the scope of this study, Author 1 contributed to the formation of the idea, literature review, engineering calculations, developing the new mathematical model, laboratory tests and obtaining the data, evaluating the data and the results. Author 2 contributed to developing the new mathematical model, evaluating the data and the results, and reviewing the paper.

7 Ethics committee approval and conflict of interest statement

There is no need to obtain permission from the ethics committee for the article prepared. There is no conflict of interest with any person/institution in the article prepared.

8 References

[1] Ehrich F. Harris' Shock and Vibration Handbook, Edition 5. Ed: Cyril M. Harris, Allan G. Piersol, McGraw-Hill Book Company, Inc., New York, 2002, 1456.
[2] Swanson E, Powell CD, Weissman S. A practical review of rotating machinery critical speeds and modes. Sound and Vibration. 2005, 39, 10-17.
[3] Iwatsubo T and Saigo M. Transverse Vibration of a Rotor System Driven by a Cardan Joint. Journal of Sound and Vibration. 1984, 95, 9-18.
[4] Seherr-Thoss HC, Schmelz F, Aucktor E. Universal Joints and Driveshafts. Springer, Berlin, 2006, 366.
[5] International Standard ISO 281. Rolling bearings- Dynamic load ratings and rating life. International Organization for Standardization. 2007.
[6] Liao NT, Lin JF. A New Method Developed for the Analysis of Ball Bearing Fatigue Life Considering Variable Contact Angles. Tribology Transactions. 2008, 46 (3), 435-446.
[7] Goodman J. Roller and Ball Bearings. Minutes of the Proceedings of the Institution of Civil Engineers. 1912, 189, 82-127.
[8] Zaretsky EV. A. Palmgren Revisited-A Basis for Bearing Life Prediction. Society of Tribologists and Lubrication Engineers. 1998, 54 (2), 18-24.
[9] Lundberg G, Palmgren A. Dynamic Capacity of Rolling Bearings. Acta Polytechnica, Mechanical Engineering Series. 1947, 1 (3), 7.
[10] Lundberg G, Palmgren A. Dynamic Capacity of Rolling Bearings. Acta Polytechnica, Mechanical Engineering Series. 1952, 2 (4), 96–127.
[11] ISO 281:1990. Rolling bearing- Dynamic load ratios and rating life. International Organization for Standards, Geneva, 1990.
[12] ANSI/AFBMA 9. Load rating and fatigue life for ball bearings. The Anti-Friction Bearing Manufacturers Association, Washington, DC, USA, 1990.
[13] Ioannides E, Harris TA. A New Fatigue Life Model for Roiling Bearings. Journal of Tribology. 1985, 107(3), 367-377.
[14] Zaretsky EV. Fatigue Criterion to System Design, Life and Reliability. Trans. AIAA, Journal of Propulsion and Power. 1987, 3 (1), 76-83.
[15] Zaretsky EV, Poplawski JV, Peters SM. Comparison of Life Theories for Rolling-Element Bearings. Tribology Transactions. 1996, 39 (2), 501-503.
[16] Ebert FJ, Poulin P. The Effect of Cleanliness on the Attainable Bearing Life in Aerospace Applications. Tribology Transactions. 1995, 38 (4), 851-856.
[17] Losch T, Weigland M. The Calculation of Fatigue-Life of Rolling Bearings Depending on their Operating Conditions. Ed: R. Bamsby, ASME 95-TRIB-58, 1995, Orlando, USA.
[18] Takata H. Possibility of a new method for calculating fatigue life for rolling bearings. Japanese J. of Tribology. 1994, 36 (6), 707-718.
[19] Talcata H, Furumura K, Murakami Y. Development of a new method for estimating the fatigue life of rolling Bearings. ASME/STLE Tribology Conference (Bildiri kitabı), Orlando, USA, 1995, 11-16.
[20] Tallian TE. A Data-Fitted Rolling Bearing Life Prediction Part I: Mathematical Model. 1996, 39 (2), 249-258.
[21] Tallian TE. A Data-Fitted Rolling Bearing Life Prediction Part II: Model Fit to the Historical Experimental Database. Tribology Transactions. 1996, 39 (2), 259-268.
[22] Tallian TE. A Data-Fitted Rolling Bearing Life Prediction Model-Part III: Parametric Study, Comparison to Published Models and Engineering Review. Tribology Transactions. 1996, 39 (2), 269-275.
[23] Zaretsky EV, Poplawski JV, Miller CR. Rolling Bearing Life Prediction-Past, Present, and Future. National Aeronautics and Space Administration Glenn Research Center, NASA/TM-2000-210529. 2000, 7.
[24] Zaretsky EV. Rolling bearing life prediction, theory, and application. Recent Developments in Wear Prevention, Friction and Lubrication. 2010, 45-136.
[25] Zaretsky EV. In Search of A Fatique Limit: A Critique of ISO Standard 281:2007. Tribology and Lubrication Technology, August-2010, 30-40.
[26] International Standard ISO-76:1987. Rolling Bearings–Static Load Ratings. International Organization for Standardization. 1987, Geneva, Switzerland.
[27] KOYO, High Wing Series Drive Shafts. JTEKT Corparation, Japan. Cat. No. B2022E, 30.
[28] Harris TA, Kotzalas MN. Rolling Bearing Analysis Vol. 1. CRC Press, Boca Raton, FL, 2007.
[29] Harris TA, Kotzalas MN. Rolling Bearing Analysis. Vol. 2. CRC Press, Boca Raton, FL, 2007.
[30] Stribeck R. Ball Bearing for Various Loads. Transactions of the ASME. 1907, 29, 420-463.
[31] Sadeghi F, Jalalahmadi B, Slack TS, Raje N, Arakere NK. A Review of Rolling Contact Fatigue. ASME Journal of Tribology. 2009, 131 (4), 1-15.
[32] Oswald FB, Zaretsky EV, Poplawsky JV. Effect of Internal Clearance on Load Distribution and Life of Radially Loaded Ball and Roller Bearings. Tribology Transactions. 2012, 55 (2), 245-265.
[33] Belorit M, Hrcek S, Smetanka L. Mathematical Algorithm for Calculating An Optimal Axial Preload of Rolling Bearings with The Respect to Their Life. IOP Conf. Series: Materials Science and Engineering. 2018, 393. DOI: 10.1088/1757-899X/393/1/012055.
[34] Johnson KL. Contact Mechanics. Cambridge University Press, London, Great Britain, 1994, 452.
[35] Hertz H. On The Contact of Solids- On The Contact of Rigid Elastic Solids and on Hardness. Miscellaneous Papers, Macmillan and Co. Ltd., London, England, 1896, 146-183.

Düzeltme Öncesi - Uncorrected Version

Herkese Açık

[36] Radzimovsky E. Stress Distribution and Strength Condition of Two Rolling Cylinders Pressed Together. University of Illinois Bulletin. 1953, 50 (44).
[37] Sackfield A, Hills DA. Some useful results in the classical Hertz contact problem. The Journal of Strain Analysis for Engineering Design. 1983, 18, 101-105.
[38] Romanowicz P, Szybiński B. Estimation of maximum fatigue loads and bearing life in ball bearings using multi-axial high-cycle fatigue criterion. Applied Mechanics and Materials. 2014, 621, 95-100.
[39] Burden RL, Faires JD. Numerical Analysis 9th Edition. Brooks/Cole Cengage Learning, Boston, USA, 2010, 888.

Düzenlenmemiş Sürüm - Uncorrected Version